

The 2015 Mw7.8 Gorkha, Nepal earthquake: Earthquake relocation, seismogenic structure and prospective seismic risk

Ling Bai¹, Guohui Li², Md Moklesur Rahman³, Hui Su⁴

1. Corresponding Author. Professor, Institute of Tibetan Plateau Research, Chinese Academy of Sciences, No. 16 Lincui Road, Chaoyang District, Beijing, China.
Email: bailing@itpcas.ac.cn
2. Ph.D student, Institute of Tibetan Plateau Research, Chinese Academy of Sciences, No. 16 Lincui Road, Chaoyang District, Beijing, China.
Email: liguohui@itpcas.ac.cn
3. Ph.D student, Institute of Tibetan Plateau Research, Chinese Academy of Sciences, No. 16 Lincui Road, Chaoyang District, Beijing, China.
Email: moklesh@itpcas.ac.cn
4. Graduate student, College of Geophysics and Information Engineering, China University of Petroleum, No. 18 Fuxue Rd., Changping District, Beijing, China.
Email: 1135866801@qq.com

Abstract

The 25 April 2015, Mw7.8 Gorkha, Nepal, earthquake ruptured a shallow section of the Indian-Eurasian plate boundary by reverse faulting with NNE-SSW compression, consistent with the direction of current Indian-Eurasian continental collision. The Gorkha main shock and aftershocks were recorded by permanent global and regional arrays and by a temporary local broadband array near the China-Nepal border deployed prior to the Gorkha main shock. Here we relocated the 2015 Gorkha aftershocks and performed probabilistic seismic hazard assessment. The main shock is located on the horizontal MHT at a depth of 18.5 km. Aftershocks show faulting structure in the hanging wall above the MHT. There are significant spatial variations in seismic hazard levels. The regions along the Main Central Thrust from east to west appear exposed to high seismic hazard levels.

Keywords: The 2015 Mw 7.8 Gorkha earthquake; China-Nepal broadband seismic Array; Source parameter; Crustal structure; Seismic hazard analysis

1. Introduction

The Himalaya orogenic belt is one of the most representative continental collision zones on Earth. It is also a key region for seismological studies on the mechanism of plate boundary megathrust earthquakes and the evaluation of the associated seismic hazards. The region is classically divided into four tectonic units from south to north: Sub-Himalaya, Lesser Himalaya, Higher Himalaya, and Tethyan Himalaya (Figure 1). The Main Frontal Thrust (MFT), Main Boundary Thrust (MBT), Main Central Thrust (MCT), and South Tibet Detachment (STD) separate the four

tectonic units. They converge at the Main Himalaya Thrust (MHT), the detachment along which the Indian plate subducts beneath the Himalayan Mountains (Ni and Barazangi, 1984; Zhao et al., 1993; Nabelek et al., 2009).

The potential for devastating earthquakes in the Himalaya has long been recognized. Historical documents since the tenth century show evidence for great Himalayan earthquakes with a recurrence interval of about 800 years (Kumar et al., 2010; Bollinger et al., 2014). Nearly 500 earthquakes of $M_w \geq 4.5$ have occurred along the Himalayas orogen since 1964. The 2015 $M_w 7.8$ Gorkha earthquake is the largest earthquake that has occurred along the Himalaya since digital earthquake recordings have become available. The earthquake affected many nearby countries, caused nearly 9000 deaths, destroyed many of the infrastructures in the source area (Figure 2). We deployed a broadband array along the China-Nepal border before this earthquake. The main shock and most aftershocks are located within 0-300 km from the array.

In this study, we combine our data with the permanent short-period network of Nepal, and the broadband seismic network of Tibet, China earthquake administration to form a comprehensive dataset of the aftershock recordings. We use various data processing techniques to study the 3D geometry of the Main Himalaya Thrust faulting system and the prospective seismic risk in Nepal. This study provides new constraints on the collision and uplift processes for the Himalaya orogenic belt and the mitigation of earthquake disasters that affect the economic and social development of the region.

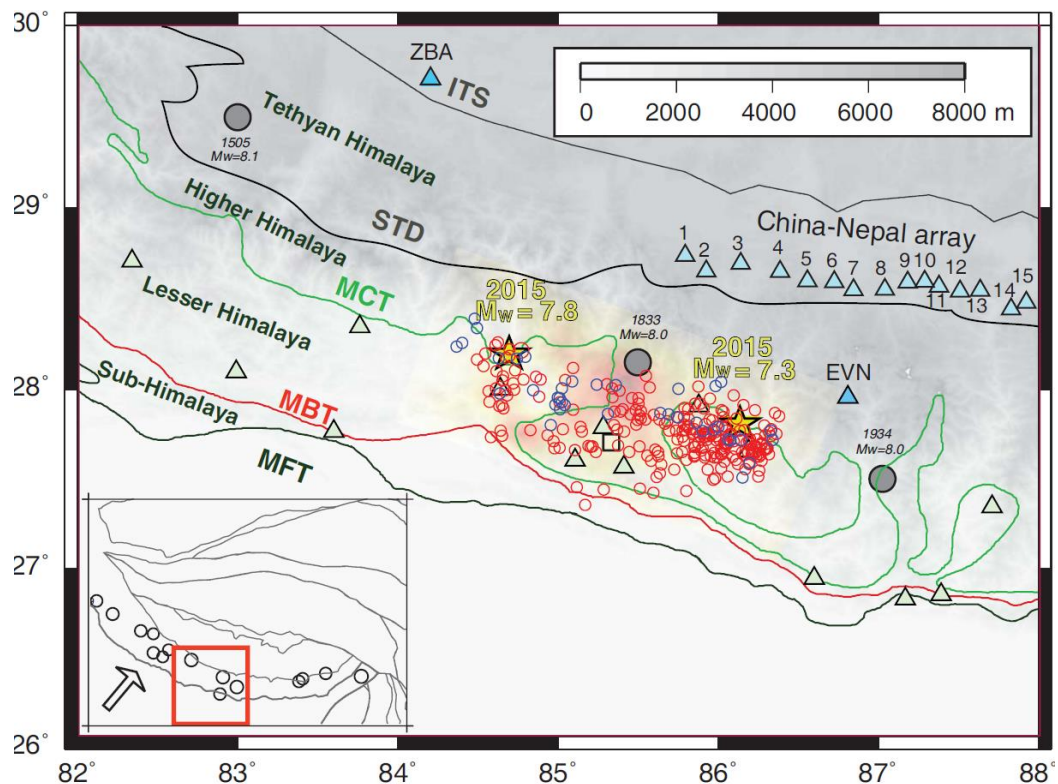


Figure 1. The relocations of the $M_w 7.8$ Gorkha, $M_w 7.3$ Kodari earthquakes (yellow stars), and aftershocks within one month. Blue triangles show the 15 stations of the China-Nepal seismograph array deployed before the Gorkha earthquake. The inset a the lower left corner shows historic seismicity of $M_w \geq 7.5$ since 1000. MFT: Main Frontal Thrust, MBT: Main Boundary Thrust, MCT: Main Central Thrust, STD: South Tibetan Detachment, ITS: Indus-Tsangpo suture.



Figure 2. Damaged structures of (left) the Boudha Stupa in the eastern Kathmandu Valley and (right) a house near Swayambhunath Stupa in the western Kathmandu Valley (photographs were taken in April, 2016, one year after the Gorkha Earthquake).

2. Data and methods

We collect waveform data from the China-Nepal array, the China National Seismic Network (CNSN), and the Global Seismic Network. Bulletin data are taken from the National seismological centre of Nepal, the International Seismological Centre (ISC), the National Earthquake Information Center (NEIC) of the U.S. Geological Survey, and the National Oceanic and Atmospheric Administration (NOAA). Our local temporary array recorded most of the aftershocks at epicentral distances less than 300 km. Permanent seismic stations in the Tibetan region at epicentral distances of 2-7° recorded clear Pn and Sn head waves and Pg and Sg direct waves. At teleseismic distances, surface reflections pP and sP phases for moderate earthquakes provide constraints on focal depths.

We determine hypocentre of the main shock and aftershocks using a multi-scale double-difference earthquake relocation method (Multi-DD) (Bai and Zhang, 2015; Bai et al., 2016), which is modified from the hypoDD programs (Waldhauser, 2001) to include phases recorded by regional and teleseismic networks. Since differential traveltimes do not depend strongly on the assumed velocity models along the whole ray path (Waldhauser and Ellsworth, 2000; Waldhauser and Schaff, 2007), the joint analysis of local, regional, and teleseismic data and the precise measurements of differential phase arrival times via waveform cross correction for the China-Nepal array improve the relative focal depth determinations considerably.

To estimate the seismic hazards for future earthquakes that may occur in Nepal, we used the seismic hazard module CRISIS2015 (Ordaz et al., 2015) because of its high efficiency of calculation and flexibility in model selection (Danciu et al., 2010). We estimated the hazard values using 18 different methods and combined them together using the logic tree structure to obtain the final value.

3. Results

The average focal depth after relocation is 14.7 km below the surface, deeper than the default value of 10 km in the NEIC catalog for most of the aftershocks. Almost all aftershocks occurred to the southeast of the main shock. Few aftershocks occurred northeast of Kathmandu, where coseismic slip is large (Avouac et al., 2015; Fan and Shearer, 2015; Lindsey et al., 2015; Wang et al., 2015; Wang and Fialko, 2015). The Mw7.3 Kodari earthquake occurred on the eastern edge of the aftershock zone (Figure 1). We estimate the focal depth of the main shock to be 18.5 ± 2 km, consistent with the depth of the MHT (Nabelek et al., 2009) and the locking line at the source region (Bilham et al., 2001; Avouac et al., 2015).

Figure 3 shows relocated hypocenters of the main shock and major aftershocks

along a N20° E cross section perpendicular to the strike of the Gorkha main shock fault plane. Most aftershocks are shallower than the main shock and located in the hanging wall. They line up as clear north dipping structures with dip angles of about 25°, which is 15° steeper than the dip of the MHT (Nabelek et al., 2009) and the shallow nodal plane of the main shock (Avouac et al., 2015). The steeper dips are in good agreement with the focal mechanism solutions of several aftershocks reported in the global centroid moment tensor (gCMT) catalog.

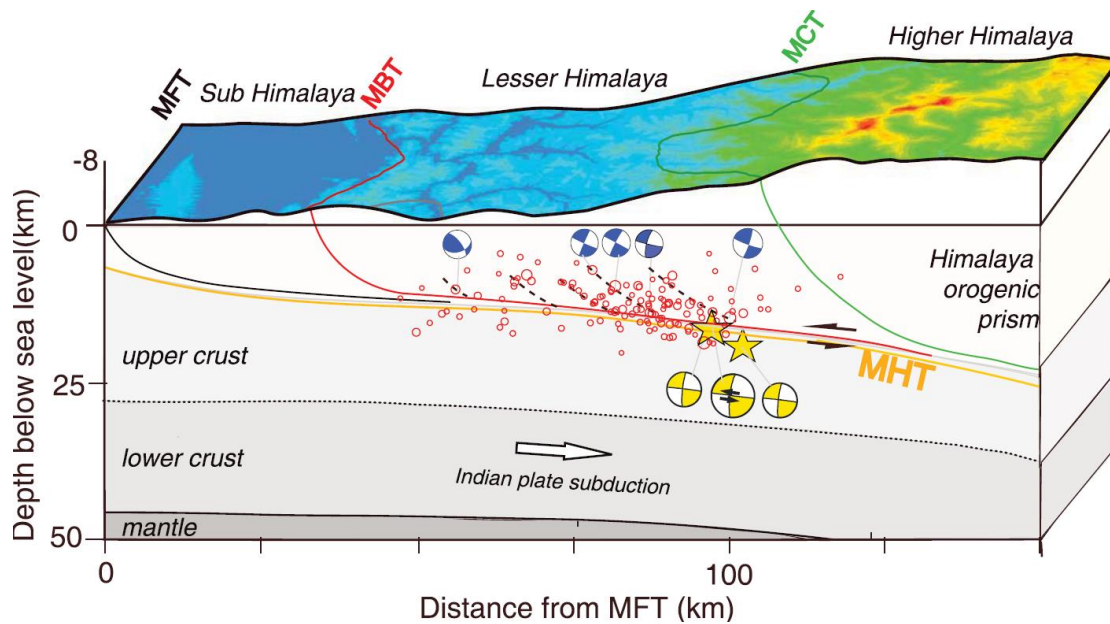


Figure 3. Cross section showing relocated earthquakes. Yellow and blue earthquake focal mechanisms show events in cross-sectional view with dip angles of about 10° and 25°, respectively (<http://www.globalcmt.org/>). The dotted black lines indicate the steeply dipping faults where aftershocks occurred within the Lesser Himalayan thrust system.

The probabilistic seismic hazard assessment (PSHA) process was performed by dividing the entire region into small grids of size $0.1^\circ \times 0.1^\circ$. The total number of grid cells was 5000, and the hazard value at the center of each cell was calculated by considering all of the sources within a radius of 300 km. This calculation was performed by disaggregating the hypocentral distance into small intervals of 1 km, and the magnitude range (between the minimum and maximum magnitude) into small incremental values of 0.1.

The spatial variation in peak ground acceleration (PGA) estimated for a 2% probability of exceedance over 50 years (Figure 4) ranged between 0.20 g and 0.92 g. The clustering of hazard values produced two clearly distinguishable zones: the central segment of Nepal elongated from east (Dhankuta) to west (Darchula), characterized by a high hazard level with a maximum value of 0.92 g (around the Kathmandu Valley); and the southern region along the Nepal-India boundary with remarkably low hazard levels (~0.20 g). The Gorkha and Rukum areas were also calculated to have moderate hazard values.

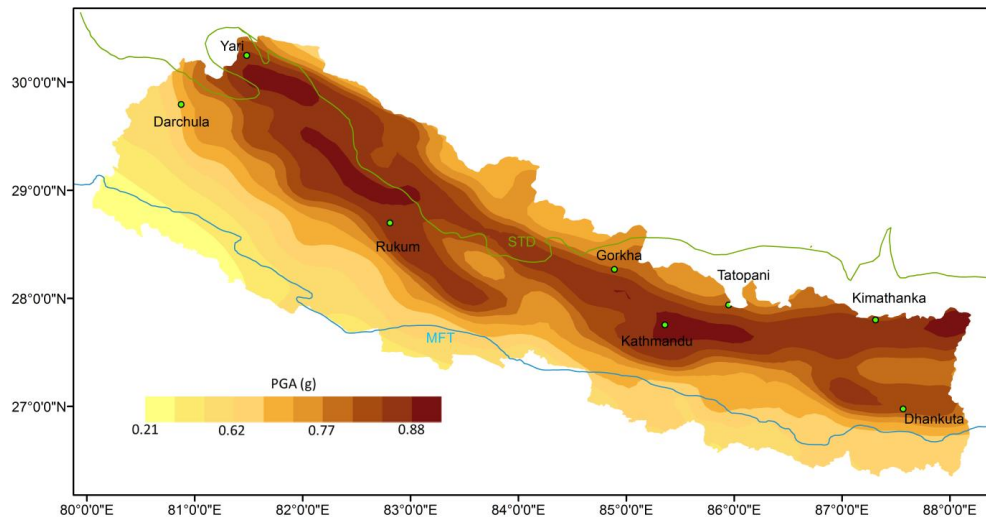


Figure 4. Spatial variation in PGA estimated for a 2% probability of exceedance over 50 years.

4. Discussion and conclusions

While the main shock ruptured a section of the MHT, most of the aftershocks have shallower focal depths and the northward dipping nodal planes of the largest aftershocks have larger dip angles. We infer therefore that the aftershocks are mainly distributed on steeper dipping structures within the hanging wall of the Lesser Himalaya. Active faults exist throughout the Kathmandu basin. However, strike-slip earthquakes on these near-vertical faults have not been recorded in the past 50 years (Bai et al., 2015). Great earthquakes in the past 200 years have been attributed to slip on the MHT. Many of the historical large earthquakes along the Himalaya orogeny were located beneath the Lesser Himalaya (Rajendran et al., 2015). We infer that the Lesser Himalaya thrust system is the most seismically active region along the Himalaya convergence and accommodates most of the elastic strain accumulation of the region.

Seismic hazard values in Nepal vary significantly from place to place. The Lesser Himalaya between MCT and MBT is seismically the most active region along the Himalayan convergence. The high rate of elastic strain accumulation along the Himalayan convergence (Ader et al., 2012), combined with the fully locked MHT (Stevens and Avouac, 2015), cause the central segment of the Himalaya (Nepal) to experience a high seismic hazard potential. The partial release of this accumulated strain, as rooted into the core of the MHT, by the Gorkha Earthquake of 2015 has only heightened the likelihood of central Nepal facing devastating earthquakes in the near future. However, the lateral variation in hazard levels along the central Himalaya is significant. Our estimated hazard values provide new constraints for structural engineers for the seismic design load analysis of buildings.

Acknowledgements

This research was supported by the grants of the National Nature Science Foundation of China (Nos. 41274086 and 41490611) and the Chinese Academy of Sciences (CAS: L. Bai).

References

- Ader T., Avouac J.P., Liu-Zeng J., Lyon-Caen H., Bollinger L., Galetzka J., Genrich J., Thomas M., Chanard K., Sapkota S.N., Rajaure S., Shrestha P., Ding L., Flouzat M., (2012) Convergence rate across the Nepal Himalaya and interseismic coupling on the Main Himalayan Thrust: Implications for seismic hazard. *J. Geophys. Res.* 117: B04403, doi:10.1029/2011JB009071.

- Bai, L., Li, G., Khan, N.G., Zhao, J., and Ding, L., (2015) Focal depths and mechanisms of shallow earthquakes in the Himalayan-Tibetan region, *Gondwana Res.*, doi: 10.1016/j.gr.2015.07.009.
- Bai, L., and Zhang, T., (2015) Complex deformation pattern of the Pamir-Hindu Kush region inferred from multi-scale double-difference earthquake relocations, *Tectonophysics*, 638, 177-184, doi:10.1016/j.tecto.2014.11.006.
- Bai, L., Liu, H., Ritsema, J., Mori, J., Zhang, T., Ishikawa, Y., Li, G., (2016) Faulting structure above the Main Himalayan Thrust as shown by relocated aftershocks of the 2015 Mw 7.8 Gorkha, Nepal earthquake, *Geophys. Res. Lett.*, 43, 637-642, doi:10.1002/2015GL066473.
- Bilham, R., Gaur, V., Molnar, P., (2001) Himalayan seismic hazard, *Science*, 293, 1442-1444.
- Bollinger, L., Sapkota, S.N., Tapponnier, P., Klinger, Y., Rizza, M., Van der Woerd, J., Tiwari, D.R., Pandey, R., Bitri, A., Bes de Berc, S., (2014) Estimating the return times of great Himalayan earthquakes in eastern Nepal: Evidence from the Patu and Bardibas strands of the Main Frontal Thrust, *J. Geophys. Res. Solid Earth*, 119, 7123-7163, doi:10.1002/2014JB010970.
- Danciu L, Monelli D., Pagani M., Wiemer S., (2010) GEM1 Hazard: Review of PSHA software, GEM Technical Report 2010-2, GEM Foundation, Pavia, Italy.
- Fan, W., Shearer, P.M., (2015) Detailed rupture imaging of the 25 April 2015 Nepal earthquake using teleseismic P waves, *Geophys. Res. Lett.*, 42, 5744-5752, doi:10.1002/2015GL064587.
- Kumar, S., Wesnousky, S.G., Jayangondaperumal, R., Nakata, T., Kumahara, Y., Singh, V., (2010) Paleoseismological evidence of surface faulting along the northeastern Himalayan front, India: Timing, size, and spatial extent of great earthquakes, *J. Geophys. Res.*, 115, B12422, doi:10.1029/2009JB006789.
- Lindsey, E.O., Natsuaki, R., Xu, X., Shimada, M., Hashimoto, M., Melgar, D., Sandwell, D.T., (2015) Line of sight displacement from ALOS-2 interferometry: Mw 7.8 Gorkha earthquake and Mw 7.3 aftershock, *Geophys. Res. Lett.*, 42, 6655-6661, doi:10.1002/2015GL065385.
- Nabelek, J., Hetenyi, G., Vergne, J., Sapkota, S., Kafle, B., Jiang, M., Su, H., Chen, J., Huang, B., H.-C. Team, (2009) Underplating in the Himalaya-Tibet collision zone revealed by the Hi-CLIMB experiment, *Science*, 325, 1371-1374.
- Ni, J., Barazangi, M., (1984) Seismotectonics of the Himalayan collision zone: Geometry of the underthrusting Indian plate beneath the Himalaya, *J. Geophys. Res.*, 89(B2), 1147-1163.
- Ordaz et al., (2015), CRISIS2015 version 2.2: Computer program for computing seismic hazard. Instituto de Ingenieria, UNAM, Mexico.
- Rajendran, C.P., John, B., Rajendran, K., (2015) Medieval pulse of great earthquakes in the central Himalaya: Viewing past activities on the frontal thrust, *J. Geophys. Res. Solid Earth*, 120, 1623-1641, doi:10.1002/2014JB011015.
- Stevens, V.L., Avouac, J-P., (2015) Interseismic coupling on the main Himalayan thrust. *Geophys. Res. Lett.* 42: 5828-5837, doi: 10.1002/2015GL064845.
- Waldhauser, F., (2001), hypoDD-A program to compute double-difference hypocenter locations (hypoDD version 1.0-03/2001), Open File Rep. USGS/OFR-01-113, vol. 113, US Geol. Surv., Menlo Park, Calif.
- Waldhauser, F., Ellsworth, W.L., (2000) A double-difference earthquake location algorithm: Method and application to the northern Hayward fault, California, *Bull. Seismol. Soc. Am.*, 90(6), 1353-1368.
- Waldhauser, F., Schaff, D., (2007) Regional and teleseismic double-difference earthquake relocation using waveform cross-correlation and global bulletin data, *J. Geophys. Res.*, 112, B12301, doi:10.1029/2007JB004938.
- Wang, K., Fialko, Y., (2015) Slip model of the 2015 Mw7.8 Gorkha (Nepal) earthquake from inversions of ALOS-2 and GPS data, *Geophys. Res. Lett.*, 42, 7452-7458, doi:10.1002/2015GL065201.
- Wang, W., Hao, J., He, J., Yao, Z., (2015) Rupture process of the Mw7.9 Nepal earthquake April 25, 2015, *Sci. China Earth Sci.*, 58, 1895-1900, doi:10.1007/s11430-015-5170-y.
- Zhao, W., Nelson, K.D., and Project INDEPTH Team, (1993) Deep seismic reflection evidence for continental underthrusting beneath southern Tibet, *Nature*, 366, 557-559.